

Materials properties of out-of-plane heterostructures of MoS₂-WSe₂ and WS₂-MoSe₂

Bin Amin

Department of Physics, Hazara University, Mansehra, Karakoram Hwy, Dhodial 21120, Pakistan

Thaneshwor P. Kaloni, Georg Schreckenbach, and Michael S. Freund

Department of Chemistry, University of Manitoba, Winnipeg, Manitoba R3T 2N2, Canada

Abstract

Based on first-principles calculations, the materials properties (structural, electronic, vibrational, and optical properties) of out-of-plane heterostructures formed from the transition metal dichalcogenides, specifically MoS₂-WSe₂ and WS₂-MoSe₂ were investigated. The heterostructures of MoS₂-WSe₂ and WS₂-MoSe₂ are found to be direct and indirect band gap semiconductors, respectively. However, a direct band gap in the WS₂-MoSe₂ heterostructure can be achieved by applying compressive strain. Furthermore, the excitonic peaks in both monolayer and bilayer heterostructures are calculated to understand the optical behavior of these systems. The suppression of the optical spectrum with respect to the corresponding monolayers is due to interlayer charge transfer. The stability of the systems under study is confirmed by performing phonon spectrum calculations.

Transition metal dichalcogenides (TMDCs) are promising materials for various applications [1–5], for example field-effect transistors. Quantum confinement in these semiconductors going from bulk to monolayer results in the transition from indirect to direct band gap semiconductor, which makes them superior in nano-electronics applications as compared to the well studied material graphene that has no band gap.[6–14] In addition, due to their distinct electronic properties, TMDC monolayers have been utilized in logic circuits [15] as well as in memory devices.[16]

Stacking of TMDCs monolayers in order to form heterostructures with van der Waals interactions enables the creation of atomically sharp interfaces [17], and also provides a route to a wide variety of semiconductor heterojunctions with interesting properties.[18] Type-II band alignment in these heterostructures has been demonstrated, which reduces the overlap between the electron and hole wave functions by slowing down the charge recombination, which in fact is expected to be an efficient way for light detection and harvesting.[17, 19] Recently, the long-lived interlayer excitons have been investigated in the MoSe₂-WSe₂ heterostructure, which indeed opens the large avenue for light-emitting diodes and photovoltaic devices.[20]. The structural, electronic, photocatalytic, and optical properties of out-of-plane and in-plane heterostructures of TMDCs have been investigated by employing first-principles calculations.[21] It has been demonstrated that all the out-of-plane heterostructures show an indirect band gap with type-II band alignment. However, a direct band gap can be obtained by the application of tensile strain in specific cases, such as the heterostructures of MoSe₂-WSe₂ and MoTe₂-WTe₂. It has also been predicted by theoretical calculations that the direct band gaped bilayer can be generated by alteration of the individual monolayers of TMDCs in the heterostructures.[22]

A vertical heterostructure of MoS₂-WSe₂ has been fabricated by stacking of MoS₂ and WSe₂ monolayers.[23] Based on the shifts observed in the Raman and photoluminescence spectra, it has been found that thermal in-

teractions enhance the coupling between the two monolayers. An atomically thin *p-n* junction diode has been synthesized from a stacked MoS₂-WSe₂ heterojunction. It shows an excellent current rectification and rapid photo-response with a high quantum efficiency.[24] Lee et al. [25] also fabricated atomically thin *p-n* heterojunctions from MoS₂ and WSe₂ monolayers and demonstrated that the tunneling-assisted coupling between MoS₂ and WSe₂ layers is responsible for the tunability of the electronic and optoelectronic responses. The van der Waals heterostructures of MoS₂-WSe₂ and MoS₂-MoSe₂ have been demonstrated using ultra-low frequency Raman spectroscopy.[26] It has been shown that a special Raman feature arises from the layer-breathing mode vibration between two incommensurate monolayers. Due to the charge transfer across the interface of the MoS₂ and WSe₂ heterostructures, a photovoltaic effect has been observed.[27] Furthermore, a high gate coupling efficiency of about 80% has been demonstrated for tuning the band offsets at the MoS₂-WSe₂ vertical interface in dual-gate device.[28]

However, the structural and electronic properties of such heterostructures are not well understood. Therefore, in the present work, comprehensive insight is gained into the physical properties of the MoS₂-WSe₂ and WS₂-MoSe₂ heterostructures that are investigated with/without biaxial compressive strain using density functional theory calculations (see supplementary material).[29] The reduction of the optical spectrum with respect to the corresponding monolayers is analyzed. Furthermore, the stability of the systems under consideration is confirmed by means of the phonon spectrum.

The out-of-plane heterostructures were created by using the average of the experimental lattice constant of the constituent monolayers and by keeping one layer on top of the other such that the S/Se atoms of one layer sit on top of the W/Mo of the other layer [22], see Fig. 1. We have also cross-checked the heterostructures by using the lattice parameters of the constituent monolayers individually. After the relaxation of both the lattice constant and positions, the lattice parameter optimized to the average

	MoS ₂ -WSe ₂	WS ₂ -MoSe ₂	MoS ₂ -WSe ₂	WS ₂ -MoSe ₂
	PBE		HSE06	
a (Å)	3.25	3.25	3.22	3.22
$d_{spacing}$	3.37	3.36	3.33	3.34
X-S (Å)	2.43	2.43	2.40	2.40
X-Se (Å)	2.53	2.52	2.50	2.50
E_b (eV)	-0.20	-0.21	-0.24	-0.25
E_g (eV)	0.33	0.87	0.94	1.58
Δ_{VB} (eV)	0.46	0.19	0.44	0.18
Δ_{CB} (eV)	0.003	0.019	0.026	0.035

TABLE I: Lattice constant, interlayer spacing, bond lengths (X=Mo, W), binding energy, band gap, and band splitting (valence and conduction bands) for the out-of-plane heterostructures.

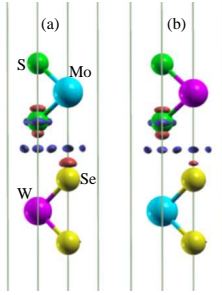


FIG. 1: Charge density difference isosurfaces for (a) MoS₂-WSe₂ and (b) WS₂-MoSe₂ heterostructures with an isovalue of 0.001 eV/Å, where red and blue color represent positive and negative charges, respectively.

value of the corresponding monolayers, as summarized in Table I. In principle, the PBE calculations overestimate, while HSE06 calculation give the correct value to the average of the experimental lattice constant of individual monolayers in corresponding heterostructures.[30] Hence, after relaxation the MoSe₂ and WSe₂ monolayers suffered from 1.8% compressive strain, while the MoS₂ and WS₂ monolayers suffered from the same amount of tensile strain in agreement with Ref. [23]. The obtained value of the interlayer spacing agrees well with experimentally and theoretically obtained values for heterostructures made of MoS₂ and WS₂ and graphene and WS₂ or WSe₂. [31, 32] The calculated bond lengths presented in Table I for both MoS₂-WS₂ and WS₂-MoSe₂ agree well with those of the corresponding monolayers (Ref. [33]) inferring weak van der Waals interactions between monolayers in the heterostructures.

The binding energies were obtained as $E = E_{\text{MoX}_2\text{-WX}_2} - E_{\text{MoX}_2} - E_{\text{WX}_2}$, where $E_{\text{MoX}_2\text{-WX}_2}$ (X=S, Se) is the total energy of the heterostructure, and E_{MoX_2} and E_{WX_2} are the total energies of the corresponding monolayers. The calculated binding energies presented in Table I show that the out-of-plane heterostructures have negative binding energies, which confirms that these systems are energetically favorable.

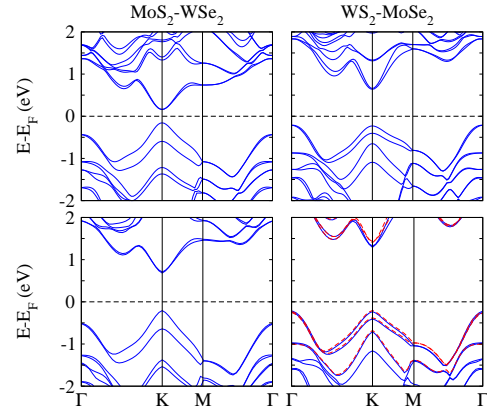


FIG. 2: Band structures of the out-of-plane heterostructures obtained using PBE (top row) and HSE06 (bottom row) functionals, where red bands are obtained under strain.

The band structures presented in Fig. 2 show that the heterostructure MoS₂-WSe₂ is a direct band gap semiconductor, while WS₂-MoSe₂ is found to be an indirect band gap semiconductor.[22] Normally, the PBE functional underestimates the band gap, therefore, the HSE06 functional is used since it has already been demonstrated that the HSE06 functional provides correct value of the band gap in terms of experimental observation.[30] The band structures shown in Fig. 2 indicate the direct and indirect band gap nature of the heterostructures of MoS₂-WSe₂ and WS₂-MoSe₂, respectively. The indirect band gap nature of the WS₂-MoSe₂ heterostructure is due to the fact that the valence band maximum (VBM) is contributed by the Mo atom, for which the spin-orbit splitting is smaller because of lower atomic number as compared to the W atom. Thus, the VBM lies at the Γ -point of the Brillouin zone.

To understand the contributions from different atomic sites, we have investigated the weighted band structure of both the heterostructures of MoS₂-WSe₂ and WS₂-MoSe₂. It is clear from Fig. 3 that the conduction band minimum (CBM) at the K-point is due to the Mo $d_{3z^2-r^2}$ orbital and the VBM at the K-point is due to the W $d_{x^2-y^2}$ and W d_{xy} orbitals of the MoS₂-WSe₂ heterostructure. This localization of the VBM and CBM in different monolayers physically separates the electron hole pairs. The strong coupling between the S/Se p orbitals and Mo/W d_{xz} and d_{yz} orbitals leads to a large splitting between their bonding and anti-bonding states, hence these orbitals do not contribute to the band edges. These results show that the VBM and CBM are contributed from different monolayers. This type of arrangement where the holes and electrons are attributed to different layers is known as type-II band alignment.[17] The homogeneous bilayers of TMDCs do not possess this net charge separation, so that an external electric field is required to achieve a type-II band alignment [35]. However, there is no electric field in our calculations for the heterostructures that nevertheless show type-II band align-

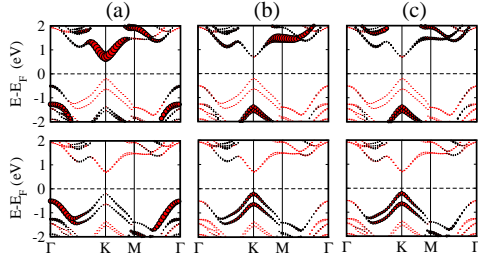


FIG. 3: Weighted bands of the MoS₂-WSe₂ out-of-plane heterostructure; Mo (first row), W (second row) for (a) $d_{3z^2-r^2}$, (b) $d_{x^2-y^2}$, and (c) d_{xy} orbitals.

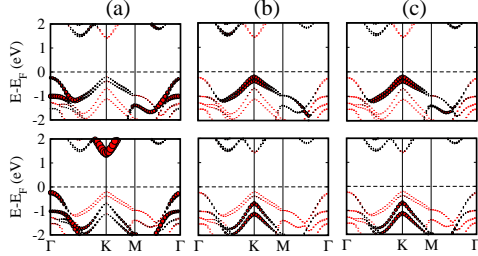


FIG. 4: Weighted bands of WS₂-MoSe₂ out-of-plane heterostructure; Mo (first row), W (second row) for (a) $d_{3z^2-r^2}$, (b) $d_{x^2-y^2}$, and (c) d_{xy} orbitals.

ment, which may be due to the intrinsic electric field that arises due to the buckled structures.[36–38]

In contrast to the MoS₂-WSe₂ heterostructure, the CBM at the K-point of the WS₂-MoSe₂ heterostructure is due to the W $d_{3z^2-r^2}$ orbital. Without applying strain, the VBM is at the Γ -point, and it is also due to the W $d_{3z^2-r^2}$ orbital with a major contribution from the Mo $d_{3z^2-r^2}$ orbital. Hence, the heterostructure of WS₂-MoSe₂ possesses a type-I band alignment, in agreement with the prediction made by Ref. [39]. Strain engineering is a widely used strategy to achieve tunable band gaps for two-dimensional materials. [40] Therefore, with the application of 0.5% compressive strain, the VB at the K-point shifts to higher energy, which is due to the Mo $d_{x^2-y^2}$ and Mo d_{xy} orbitals. Whereas, the VBM at the Γ -point shifts to lower energies. Hence, both the VBM and CBM separate the electron hole pairs to different layers and change the material to the type-II band alignment, see Fig. 4. Due to their type-II band alignment, these heterostructures can be used as active materials for fabrication of heterojunction photovoltaic devices; type-II band alignment is usually required for charge separation or formation of $p-n$ junctions.[25]

The strong spin-orbit coupling results in a significant valence band splitting (Δ_{VB}) with a minute conduction band splitting (Δ_{CB}), see Table 1. The fact is that W contributes much more to VB than Mo, and hence the VB is split. The situation is reversed for the CB, resulting in a split that is very small only, see Fig. 3. The valence band splitting in the heterostructure of MoS₂-

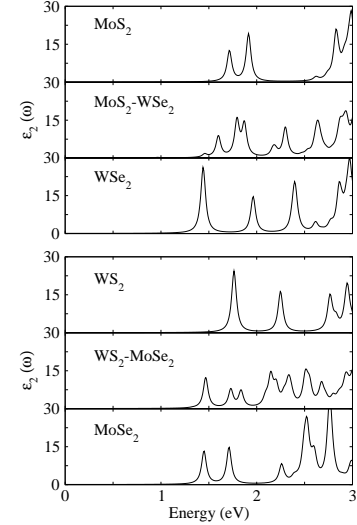


FIG. 5: Imaginary part of the dielectric function of the heterostructures in comparison with the parent monolayers as a function of photon energy.

WSe₂ was found to be larger than that of pristine MoS₂ monolayers ($\Delta_{so}^{PBE}=0.15$ eV and $\Delta_{so}^{HSE}=0.20$ eV) [33] and smaller than that of the pristine WSe₂ monolayers ($\Delta_{so}^{PBE}=0.47$ eV and $\Delta_{so}^{HSE}=0.63$ eV) [33]. The same behavior is found for the heterostructure of WS₂-MoSe₂. The splitting of the valence band (holes) and conduction band (electrons) indicates that the formation of the heterostructure is a promising route to engineer the band gap and splitting. These systems may therefore be interesting for optoelectronic and spintronic devices.[41]

Further, the imaginary parts of the dielectric function $\epsilon_2(\omega)$ of the monolayers and the heterostructures were calculated by solving the Bethe-Salpeter equation. The results presented in Fig. 5 show that the optical transitions are dominated by excitons. For monolayer MoS₂, excitonic peaks are observed at 1.77 eV and 1.92 eV, while for monolayer WSe₂ they appear at 1.50 eV and 1.96 eV. Similarly, these peaks appear at 1.77 eV and 2.24 eV for WS₂, while at 1.48 eV and 1.72 eV for monolayer MoSe₂. The position of the first excitonic peaks are in good agreement with the experimental values of MoS₂ (1.85 eV), WSe₂ (1.59 eV), WS₂, and MoSe₂ (1.56 eV).[20, 26, 42] Fig. 5 shows a systematic red shift of the excitonic peaks as the chalcogen atom becomes heavier. In general, for the red shift the band gap decreases, while for the blue shift the band gap increases [43]. We obtain exciton binding energies of 1.05 eV for MoS₂, 0.95 eV for WSe₂, 1.04 eV for WS₂, and 0.95 eV for MoSe₂ monolayers. Strong modifications of the excitons in the heterostructures with respect to the parent monolayers were found, see Fig. 5. The excitonic peaks are shifted to 1.6 eV and 1.8 eV in the case of the MoS₂-WSe₂ heterostructure, in agreement with photoluminescence spectroscopy.[26, 27] The remarkable decrease in the photoluminescence intensity of the heterostructures

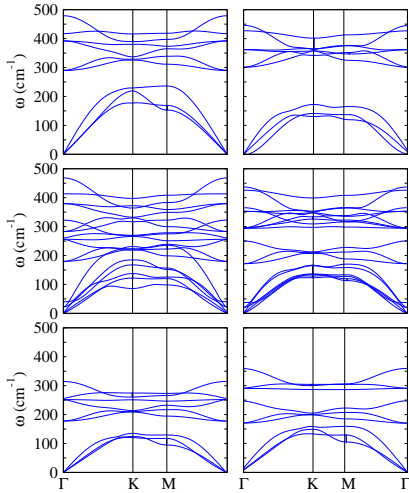


FIG. 6: Phonon spectrum for MoS₂ (top-left), WS₂ (top-right), MoS₂-WSe₂ (middle-left), WS₂-MoSe₂ (middle-right), WSe₂ (bottom-left), and MoSe₂ (bottom-right).

with respect to the parent monolayer has also been reported previously [25, 26] and is due to the efficient interlayer charge transfer. Note that, in the real experimental situation in the presence of dielectric medium, the position of an excitonic peak might change slightly.[44]

The charge transfer rate is close to the rate of exciton generation. Due to the type-II band alignment, in case of the MoS₂-WSe₂ heterostructure the photoexcited electrons in the WSe₂ layer tend to flow to the MoS₂ layer, and the holes in the MoS₂ layer tend to flow to the WSe₂ layer. The spatial separation of the electrons and holes therefore suppresses the intralayer optical recombination processes and thus the optical spectrum. To investigate the charge transfer between the constituents monolayers of the heterostructures, the charge density difference was addressed (see Fig. 1); calculated as $\Delta\rho = \rho_{MoX_2WY_2} - \rho_{MoX_2} - \rho_{WY_2}$, where $\rho_{MoX_2-WY_2}$ is the charge density of the heterostructure, ρ_{MoX_2} is the charge density of the isolated MoX₂ monolayer and ρ_{WY_2} is the charge density of the isolated WY₂ monolayer. From the Bader population analysis we have found that the S atom gains 0.008 e, while the Se atom loses 0.012 e in the MoS₂-WSe₂ heterostructure. Similarly in case of WS₂-MoSe₂ Se atoms lose 0.009 e, while S atoms gain 0.016 e, where for unstrained system this amount is 0.009 e for Se and 0.005 e for S. These results are in good agreement with the available values reported in Ref. [45], and show that the interlayer bonding of MoS₂ and WSe₂ should be rather weak and due to long-range van der Waals forces.

In Fig. 6, the calculated phonon spectra for the heterostructures of MoS₂-WSe₂ and WS₂-MoSe₂ show good agreement with the experimental data presented in Ref. [23] In the case of the MoS₂-WSe₂ heterostructure the acoustic and optical vibration modes are at the same en-

ergies as for the corresponding monolayers of WSe₂ and MoS₂. This indicates once more that there are only very small van der Waals interactions between the two layers. The phonon spectra for pristine monolayers of both MoS₂ and WSe₂ were also calculated for comparison. The characteristic bands observed at 410 cm⁻¹ and 380 cm⁻¹ are in a good agreement indeed with the experimental values of 403 cm⁻¹ and 385 cm⁻¹ [23], which are due to the A1 mode (out-of-plane vibrations) and E1 mode (in-plane vibrations), respectively, of the MoS₂ monolayer in the heterostructure. The bands at about 250 cm⁻¹ to 260 cm⁻¹ are due to the E1 and A1 modes of the monolayer of WSe₂. These bands are also in good agreement with the experimental values of E1 (248 cm⁻¹) and A1 (260 cm⁻¹).[23] The positions of these bands are also in agreement with those of the corresponding monolayers with a small red shift (shift to lower energy) with respect to isolated MoS₂ and blue shift (shift to higher energy) with respect to isolated WSe₂. [23] Both of these blue and red shifts with respect to the corresponding monolayers are due to the fact that tensile strain is induced in MoS₂ and compressive strain is induced in WSe₂ while constructing the heterostructures. The characteristic peaks are well reproduced with respect to the experiments. Although these peaks are not exactly the same as those obtained in experiment, the simulation results provide a good approximation. The positions of the bands in the heterostructure of MoS₂-WSe₂ with respect to the corresponding monolayers show that the layers are decoupled having a very small van der Waals interaction.

In summary, we have investigated the structural and electronic properties and the vibrational and optical spectra of the van der Waals heterostructures of MoS₂-WSe₂ and WS₂-MoSe₂. It was found that MoS₂-WSe₂ is a direct band gap semiconductor with type-II band alignment. In contrast to the MoS₂-WSe₂ heterostructure, the WS₂-MoSe₂ heterostructure is an indirect band gap semiconductor with type-I band alignment. A compressive strain is an efficient way to change the heterostructure of WS₂-MoSe₂ from indirect to direct band gap nature with type-II band alignment. The splitting of the valence band (holes) and conduction band (electrons) indicates that the formation of the heterostructure is a promising route to engineer the band gap and band splitting, such that these systems would be interesting for optoelectronic and spintronic devices. The reduction of the optical spectrum with respect to the corresponding monolayers is analyzed and the stability of the systems under consideration is confirmed with the help of the phonon spectrum.

GS acknowledges funding from the Natural Sciences and Engineering Council of Canada (NSERC, Discovery Grant). MSF acknowledges support by NSERC, the Canada Research Chair program, Canada Foundation for Innovation (CFI), the Manitoba Research and Innovation Fund, and the University of Manitoba.

- [1] Y. Zhao, Y. Zhang, Z. Yang, Y. Yan, and K. Sun, *Sci. Technol. Adv. Mater.* **14**, 043501 (2013).
- [2] D. J. Late, Y.-K. Huang, B. Liu, J. Acharya, S. N. Shirodkar, J. Luo, A. Yan, D. Charles, U. V. Waghmare, V. P. Dravid *et al.*, *ACS Nano* **7**, 4879 (2013).
- [3] Y. Li, H. Wang, L. Xie, Y. Liang, G. Hong, and H. Dai, *J. Am. Chem. Soc.* **133**, 7296 (2013).
- [4] M. Chhowalla, H. S. Shin, G. Eda, L.-J. Li, K. P. Loh, and H. Zhang, *Nat. Chem.* **5**, 263 (2013).
- [5] K. Xu, Z. Wang, X. Du, M. Safdar, C. Jiang, and J. He, *Nanotechnology* **24**, 465705 (2013).
- [6] T. Georgiou, R. Jalil, B. D. Belle, L. Britnell, R. V. Gorbachev, S. V. Morozov, Y. Kim, A. Gholinia, S. J. Haigh, O. Makarovsky *et al.*, *Nat. Nanotechnol.* **8**, 100 (2012).
- [7] J. He, K. Hummer, and C. Franchini, *Phys. Rev. B* **89**, 075409 (2014).
- [8] P. Zhao, D. Kiriya, A. Azcatl, C. Zhang, M. Tosun, Y.-S. Liu, M. Hettick, J. S. Kang, S. McDonnell, S. KC, *et al.*, *ACS Nano* **8**, 10808 (2014).
- [9] D. Jariwala, V. K. Sangwan, L. J. Lauhon, T. J. Marks, and M. C. Hersam, *ACS Nano* **8**, 1102 (2014).
- [10] M. Amani, D. Lien, D. Kiriya, J. Xiao, A. Azcatl, J. Noh, S. R. Madhupathy, R. Addou, S. KC, M. Dubey *et al.*, *Science* **350**, 1065 (2015).
- [11] Q. H. Wang, K. Kalantar-Zadeh, A. Kis, J. N. Coleman, and M. S. Strano, *Nature Nanotechnol.* **7**, 699 (2012).
- [12] S. KC, R. C. Longo, R. Addou, R. M. Wallace, K. Cho, *Nanotechnology* **25**, 375703 (2014).
- [13] K. F. Mak, C. Lee, J. Hone, J. Shan, and T. F. Heinz, *Phys. Rev. Lett.* **105**, 136805 (2010).
- [14] S. KC, C. Zhang, S. Hong, R. M. Wallace, K. Cho, *2D Materials* **2**, 035019 (2014).
- [15] B. Radisavljevic, M. B. Whitwick, and A. Kis, *ACS Nano* **5**, 9934 (2011).
- [16] S. Bertolazzi, D. Krasnozhon, and A. Kis, *ACS Nano* **7**, 3246 (2013).
- [17] X. Hong, J. Kim, S. F. Shi, Y. Zhang, C. Jin, Y. Sun, S. Tongay, J. Wu, Y. Zhang, and F. Wang, *Nat. Nanotechnol.* **9**, 682 (2014).
- [18] Y. Gong, J. Lin, X. Wang, G. Shi, S. Lei, Z. Lin, X. Zou, G. Ye, R. Vajtai, B. I. Yakobson *et al.*, *Nat. Mater.* **13**, 1135 (2014).
- [19] R. Bose, G. Manna, S. Janaa, and N. Pradhan, *Chem. Commun.* **50**, 3074 (2014).
- [20] P. Rivera, J. R. Schaibley, A. M. Jones, J. S. Ross, S. Wu, G. Aivazian, P. Klement, N. J. Ghimire, J. Yan, D. G. Mandrus *et al.*, *Nat. Commun.* **6**, 6242 (2015).
- [21] B. Amin, N. Singh, U. Schwingenschlöggl, *Phys. Rev. B* **92**, 075439 (2015).
- [22] H. Terrones, F. Lopez-Urias, and M. Terrones, *Sci. Rep.* **3**, 1549 (2013).
- [23] M.-H. Chiu, M.-Y. Li, W. Zhang, W.-T. Hsu, W.-H. Chang, M. Terrones, H. Terrones, and L.-Jong Li, *ACS Nano* **8**, 9649 (2014).
- [24] R. Cheng, D. Li, H. Zhou, C. Wang, A. Yin, S. Jiang, Y. Liu, Y. Chen, Y. Huang, and X. Duan, *Nano Lett.* **14**, 5590 (2014).
- [25] C.-Ho Lee, G.-H. Lee, A. M. van der Zande, W. Chen, Y. Li, M. Han, X. Cui, G. Arefe, C. Nuckolls, T. F. Heinz *et al.*, *Nat. Nanotechnol.* **9**, 676 (2014).
- [26] C. H. Lui, Z. Ye, C. Ji, K.-C. Chiu, C.-T. Chou, T. I. Andersen, C. M. Shively, H. Anderson, J.-M. Wu, T. Kidd *et al.*, *Phys. Rev. B* **91**, 165403 (2015).
- [27] M. M. Furchi, A. Pospischil, F. Libisch, J. Burgdorfer, and T. Mueller, *Nano Lett.* **14**, 4785 (2014).
- [28] T. Roy, M. Tosun, X. Cao, H. Fang, D.-H. Lien, P. Zhao, Y.-Z. Chen, Y.-L. Chueh, J. Guo, and A. Javey, *ACS Nano* **9**, 2071 (2015).
- [29] See the supplementary material at [http://dx.doi.org/..](http://dx.doi.org/) for details about the computational methods used.
- [30] Y. Zhao and D. G. Truhlar, *J. Chem. Phys.* **130**, 074103 (2009).
- [31] T. P. Kaloni, L. Kou, T. Frauenheim, and U. Schwingenschlöggl, *Appl. Phys. Lett.* **105**, 233112 (2014).
- [32] M.-H. Chiu, C. Zhang, H.-W. Shiu, C.-P. Chuu, C.-H. Chen, C.-Y. S. Chang, C.-H. Chen, M.-Y. Chou, C.-K. Shih, and L.-J. Li, *Nat. Commun.* **6**, 7666 (2015).
- [33] J. Kang, S. Tongay, J. Zhou, J. Li, and J. Wu, *Appl. Phys. Lett.* **102**, 012111 (2013).
- [34] C.-H. Chang, X. Fan, S.-H. Lin, and J.-L. Kuo, *Phys. Rev. B* **88**, 195420 (2013).
- [35] A. Ramasubramaniam, D. Naveh, and E. Towe, *Phys. Rev. B* **84**, 205325 (2011).
- [36] T. P. Kaloni, G. Schreckenbach, M. S. Freund, *J. Phys. Chem. C* **118**, 23361 (2014).
- [37] T. P. Kaloni, G. Schreckenbach, M. S. Freund, *J. Phys. Chem. C* **119**, 3979 (2015).
- [38] T. P. Kaloni, M. Modarresi, M. Tahir, M. R. Roknabadi, G. Schreckenbach, M. S. Freund, *J. Phys. Chem. C* **119**, 11896 (2015).
- [39] H. P. Komsa and A. V. Krasheninnikov, *Phys. Rev. B* **88**, 085318 (2013).
- [40] B. Amin, T. P. Kaloni, and U. Schwingenschlöggl, *RSC Adv.* **4**, 34561 (2014).
- [41] H. Ochoa and R. Roldan, *Phys. Rev. B* **87**, 245421 (2013).
- [42] A. Ramasubramaniam *Phys. Rev. B* **86**, 115409 (2012).
- [43] H. J. Trodahl, A. R. H. Preston, J. Zhong, and B. J. Ruck, *Phys. Rev. B* **76**, 085211 (2007).
- [44] Z. Li, Y. Xiao, Y. Gong, Z. Wang, Y. Kang, S. Zu, P. M. Ajayan, P. Nordlander, and Z. Fang, *ACS Nano* **9**, 10158 (2015).
- [45] X. Su, R. Zhang, C. Guo, M. Guo, and Z. Ren, *Phys. Chem. Chem. Phys.* **16**, 1393 (2014).

Materials properties of out-of-plane heterostructures of MoS₂-WSe₂ and WS₂-MoSe₂

Bin Amin

Department of Physics, Hazara University, Mansehra, Karakoram Hwy, Dhodial 21120, Pakistan

Thaneshwor P. Kaloni, Georg Schreckenbach, and Michael S. Freund

Department of Chemistry, University of Manitoba, Winnipeg, Manitoba R3T 2N2, Canada

I. COMPUTATIONAL DETAIL

Density functional theory with the Perdew-Burke-Ernzerhof (PBE) [1] and Heyd-Scuseria-Ernzerhof (HSE06) functionals [2] implemented in the VASP package were used.[3]. The Van der Waals interactions (Grimme's approach) were taken into account to optimize the geometries as well as to perform further calculations.[4] A vacuum layer of 18 Å is used to prevent artifacts due to the periodic boundary conditions. The structures were optimized until the forces and energy reached to 0.0001 eV/Å with a high plane wave cutoff of 700 eV. A $6 \times 6 \times 1$ k-mesh was used for the

optimizations. It was further refined to a $12 \times 12 \times 1$ mesh for the subsequent calculation of the electronic and vibrational properties. Relativistic effects including spin-orbit coupling are significant for the heavy elements (Mo and W) and hence, spin-orbit and relativistic pseudopotentials have been using in the calculations. In order to study the optical spectrum, the quasi-particle self-energy corrections (GW₀) approach has been used to solve the Bethe-Salpeter equation (Tamm-Dancoff approximation).[5] The 10 highest valence and 10 lowest conduction bands were taken into account in calculating the excitonic eigenstates.

-
- [1] J. P. Perdew, K. Burke, and M. Ernzerhof, Phys. Rev. Lett. **77**, 3865 (1996).
[2] J. Heyd, G. E. Scuseria, and M. Ernzerhof, J. Chem. Phys. **124**, 219906 (2006).
[3] G. Kresse and J. Hafner, Phys. Rev. B **47**, 558 (1993).

- [4] S. Grimme, J. Comput. Chem. **27**, 1787 (2006).
[5] A. Chantzis, A. D. Laurent, C. Adamo, and D. Jacquemin, J. Chem. Theory Comput. **9**, 4517 (2013).